

Atmospheric controls and long range predictability of directional waves in the United Kingdom & Ireland

T. Scott¹, G. Masselink¹, R. J. McCarroll¹, B. Castelle², G. Dodet³, A. Saulter⁴, A. A. Scaife^{4,5} and N. Dunstone⁴

¹ School of Biological and Marine Sciences, University of Plymouth, UK.

² University of Bordeaux/CNRS, UMR EPOC, Bordeaux, France.

³ IFREMER, Univ. Brest, CNRS, IRD, Laboratoire d'Océanographie Physique et Spatiale, IUEM, Brest, France.

⁴ UK Met Office, Exeter, UK

⁵ College of Engineering, Mathematics and Physical Sciences, University of Exeter, UK.

Corresponding author: Tim Scott

timothy.scott@plymouth.ac.uk

Key Points:

- Over 70% of inshore wave climates in United Kingdom and Ireland are directionally bimodal
- Combinations of winter atmospheric circulation indices NAO, WEPA, SCAND and EA are significantly correlated with directional wave climates in all regions
- Regression models using multiple winter atmospheric indices enable skillful reconstructions of directional wave climate in all regions ($r^2 = 0.45\text{--}0.8$)

Abstract

Improved understanding of how our coasts will evolve over a range of time scales (years-decades) is critical for effective and sustainable management of coastal infrastructure. Globally, sea-level rise will result in increased erosion, with more frequent and intense coastal flooding. Understanding of current and future coastal evolution requires robust knowledge of the wave climate. This includes spatial, directional and temporal variability, with recent research highlighting the importance of wave climate directionality on coastal morphological response, for example in UK, Australia and California. However, the variability of the inshore directional wave climate has received little attention, and an improved understanding could drive development of skillful seasonal or decadal forecasts of coastal response. We examine inshore wave climate at 63 locations throughout the United Kingdom and Ireland (1980–2017) and show that 73% are directionally bimodal. We find that winter-averaged expressions of six leading atmospheric indices are strongly correlated with both total and directional winter wave power (peak spectral wave direction) at all studied sites. Coastal classification through hierarchical cluster analysis and stepwise multi-linear regression of directional wave correlations with atmospheric indices defined four spatially coherent regions. We show that combinations of indices have significant skill in predicting directional wave climates ($r^2 = 0.45\text{--}0.8$; $p < 0.05$). We demonstrate for the first time the significant explanatory power of leading winter-averaged atmospheric indices for directional wave climates, and show that leading seasonal forecasts of the NAO skillfully predict wave climate in some regions.

1. Introduction

Sustainable coastal zone management requires a robust knowledge and understanding of beach and coastal dynamics over time scales ranging from years to decades. While coastal erosion is already a problem globally (Luijendijk et al., 2018; Mentaschi et al., 2018), climate change will also affect the primary drivers of coastal change, driving sea-level rise (Cazenave et al., 2014) and increased storminess in some regions of the world (Zappa et al., 2013, Scaife et al., 2012). Globally, increased sea-level rise will result in increased erosion (Le Cozannet et al., 2016), and increased frequency and intensity of coastal flooding along low-lying coasts (e.g., Voudoukas et al., 2018). A key requirement for progressing our understanding of coastal dynamics and shoreline evolution is a comprehensive knowledge of the forcing wave conditions, including its variability in space and time. The relatively recent availability of multi-decadal atmospheric sea-level pressure records (e.g., Poli et al., 2016; Antolínez et al., 2018), hindcast directional wave timeseries (e.g., Dodet et al., 2010) and beach morphological records (e.g., Masselink et al., 2016a; Turner et al., 2016; Ludka et al., 2019) have provide new insights into the importance of multi-decadal atmospheric variability in controlling inshore wave conditions and beach dynamics.

Dodet et al. (2019) investigated decadal datasets of beach morphology along the Atlantic coast of Europe and found that winter-averaged wave conditions play a key role in determining shoreline response in regions that are dominated by cross-shore exchange (on-offshore) of beach sediments on seasonal and greater timescales. Castelle et al. (2017) expanded on this and linked the variability in winter wave conditions along the Atlantic coast of Europe to winter-averaged atmospheric indices, notably the North Atlantic Oscillation (NAO; Hurrell, 1995) and the West Europe Pressure Anomaly (WEPA). It was further demonstrated that the NAO was most strongly correlated to the wave heights north of southern Ireland (52°N) and that WEPA was most strongly correlated to the wave heights from the south of Ireland to the south of Portugal. Dodet et al. (2010) demonstrated for the first time the link between the winter averaged mean wave direction variability and the winter-averaged NAO in the North East Atlantic, with positive correlations up to 0.7 in South Portugal. Martínez-Asensio et al. (2016) also examined relationships between the wind wave climate and the main climate modes of atmospheric variability (1989–2007) in the North Atlantic Ocean (including NAO, East Atlantic (EA) pattern, East Atlantic Western Russian (EA/WR) pattern and the Scandinavian (SCAND) pattern), demonstrating that NAO and EA (which has similar characteristics to WEPA) patterns are the most relevant. However, none of these studies have examined these relationships within directionally multimodal wave climates, common to more sheltered and protected seas.

Along the exposed coasts of western Europe facing the dominant wave direction, sediment movement and therefore beach response is mainly driven by cross-shore processes (Castelle et al., 2014; Masselink et al., 2016a; Scott et al., 2016; Burvingt et al., 2018). In contrast, beaches that are not directly facing the dominant wave approach, experience oblique wave approach and longshore processes drive sediment transport and beach response (Short and Masselink, 1999, Bühler and Jacobson 2001). Planform changes in beach orientation, which is referred to as “rotation” and is typical of embayed settings (Klein et al., 2002), can be driven by either spatial variability of cross-shore sediment transport, or longshore transport gradients.

Harley et al (2011) demonstrated that rotation can be linked to subtle variations in alongshore gradients of wave energy, and hence cross-shore sediment exchange, leading to out-of-phase response at embayment extremities. The most common rotation mechanism occurs in relatively sheltered settings with a mixture of distant swell and local wind wave components coming from different directions (i.e., bi-directional wave climate). In such environments, the rotational response is governed by the relative importance of the two wave directions associated with the bi-directional wave climate compared to the long-term average (Ruiz de Alegria-Arzaburu and Masselink, 2010; Bergillos et al., 2016; Wiggins et al., 2019a). Year-to-year changes in the directional variability in shoreline alignment in these settings are common, with seasonal rotational phases often leading to erosion and increased coastal vulnerability at one or other end of the embayment (e.g., Scott et al., 2016).

Recent (Pacific) basin-wide research into inter-annual wave climate variability in the Pacific (Barnard et al., 2015; Mortlock and Goodwin, 2016) revealed links between climate forcing (ENSO modes), wave direction and cross-shore beach response. Further to this, modelling work by Splinter et al. (2012) and field observations by Harley et al. (2017) have highlighted, not only the relationship between climate indices on wave direction and the subsequent impact on shoreline dynamics along the east coast of Australia, but also the impact of storm wave direction on coastal vulnerability along embayed coasts in general. In northwest Europe, research by Wiggins et al. (2019a) shows that winter-averaged variability in NAO and WEPA has significant skill in explaining wave directional balance in regions where wave climate is strongly bi-directional, as well as driving beach rotation in these regions (Wiggins et al., 2019b).

The NAO represents the principle mode of variability in the North Atlantic climate, and the skillful predictability of winter NAO is critical for long-range forecasting of the European surface winter climate (Wang et al., 2017). As an intrinsic mode of variability in atmospheric circulation, the dynamics associated to the NAO have in the past been considered unpredictable and largely stochastic in nature (Kim et al., 2012; Smith et al., 2016). But recent forecast systems (Scaife et al., 2014; Dunstone et al., 2016) have shown significant skill provided large ensembles are used (Athanasiadis et al 2016 report correlation skill of 0.86 with large multimodel ensembles) due to the anomalously weak signal-to-noise ratio of climate signals (Scaife and Smith, 2018), achieving correlation coefficients of $r > 0.6$ for winter season (DJF) forecasts initiated on 1st November. Dunstone et al. (2016) highlighted potential for further improvements in skill through increased ensemble size and decadal predictability of the NAO with large ensembles was recently reported by Smith et al. (2019). Advances have also been achieved through empirical approaches to forecasting the NAO. For example, Wang et al. (2017) used multiple linear regression of key discriminant variables (sea-ice concentration, stratospheric circulation and sea-surface temperature) and obtained forecast skill (r) of 0.69–0.71. Combined, these advances suggest that skillful prediction of seasonal and decadal coastal vulnerability may be possible (Colman et al 2011, Dobrynin et al., 2019), where forecasts of climate indices may provide a valuable tool for managing risk to society due to extreme winter-wave events, wave directional variability and corresponding geomorphological change at the coast.

An improved understanding of how leading atmospheric indices can explain seasonal to multi-decadal variability in wave power and directionality, and consequentially beach state, lays the foundation for: (1) new insights into climate controls on basin-scale coastal change; and (2)

potential exploitation of skillful season ahead and decadal forecasts of atmospheric indices. The overall aim of this paper is to investigate whether climate variability, synthesized by leading winter-averaged atmospheric indices (NAO, WEPA, EA, EA/WR, SCAND, and the Arctic Oscillation AO), significantly controls the directional balance of alongshore wave power at inshore locations throughout the UK & Ireland (UK&I), characterized by directionally bimodal (semi-) sheltered seas. The specific objectives are to: characterize the directional wave climate of the UK & Ireland (Section 3); examine relationships between winter wave climate and leading atmospheric indices (Section 4), exploring the regional coherence (Section 5); developing multi-linear regression models for predicting winter directional wave climate (Section 5); and assessing the current skill of season ahead forecasts to create useful predictions for coastal managers (Section 6).

2. Datasets

2.1 Wave modelling

The directional wave climates throughout the UK&I were analyzed at 63 coastal locations (~20m depth) using data from the UK Met Office 8-km WAVEWATCH III third-generation spectral wave model (version 3.14; Tolman, 2009), representing a 3-hourly hindcast of integrated wave parameters for the period 1980–2017. This model is described in detail by Mitchell et al. (2017) and has been extensively validated with directional buoys and satellite altimeters by Saulter (2015). These 63 sites were selected to represent all major stretches of exposed coastline throughout the UK&I (Figure 1), and range from the extremely exposed storm-dominated Atlantic west coasts of Ireland, Scotland and southwest England, to more sheltered locally-derived wind-wave dominated regions in the Irish Sea, North Sea and English Channel. Section 3 provides an overview of the annual wave climate in each region for 1980–2017.

Our analysis, including the use of peak spectral wave direction, relies on an assumption that bimodality is primarily asynchronous. A preliminary analysis indicated that synchronous bimodality, where the wave power of a secondary spectral peak is >5% that of the main peak, occurs <5% of the total time. The lowest synchronous spectral bimodality occurred in semi-sheltered coastal regions typically associated with bi-directional wave climates (S and E England). Therefore, the assumption of asynchronous bimodality is justified, and references to bimodality from herein refer to asynchronous bimodality.

2.2 Atmospheric data and climate indices

Climate indices used in this study include the leading monthly teleconnection indices (NAO, EA, EA/WR and SCAND) derived from rotated EOF analysis of the monthly mean standardized 500-mb height anomalies in the Northern Hemisphere, as described in Barnston and Livezey (1987) and available for the period 1980–2017 (downloaded from the National Oceanic and Atmospheric Administration (NOAA) Climate Prediction Center; www.cpc.ncep.noaa.gov). In addition, we used the Western Europe Pressure Anomaly (WEPA), a climate index developed by Castelle et al. (2017) and computed as the normalized sea level pressure (SLP) gradient

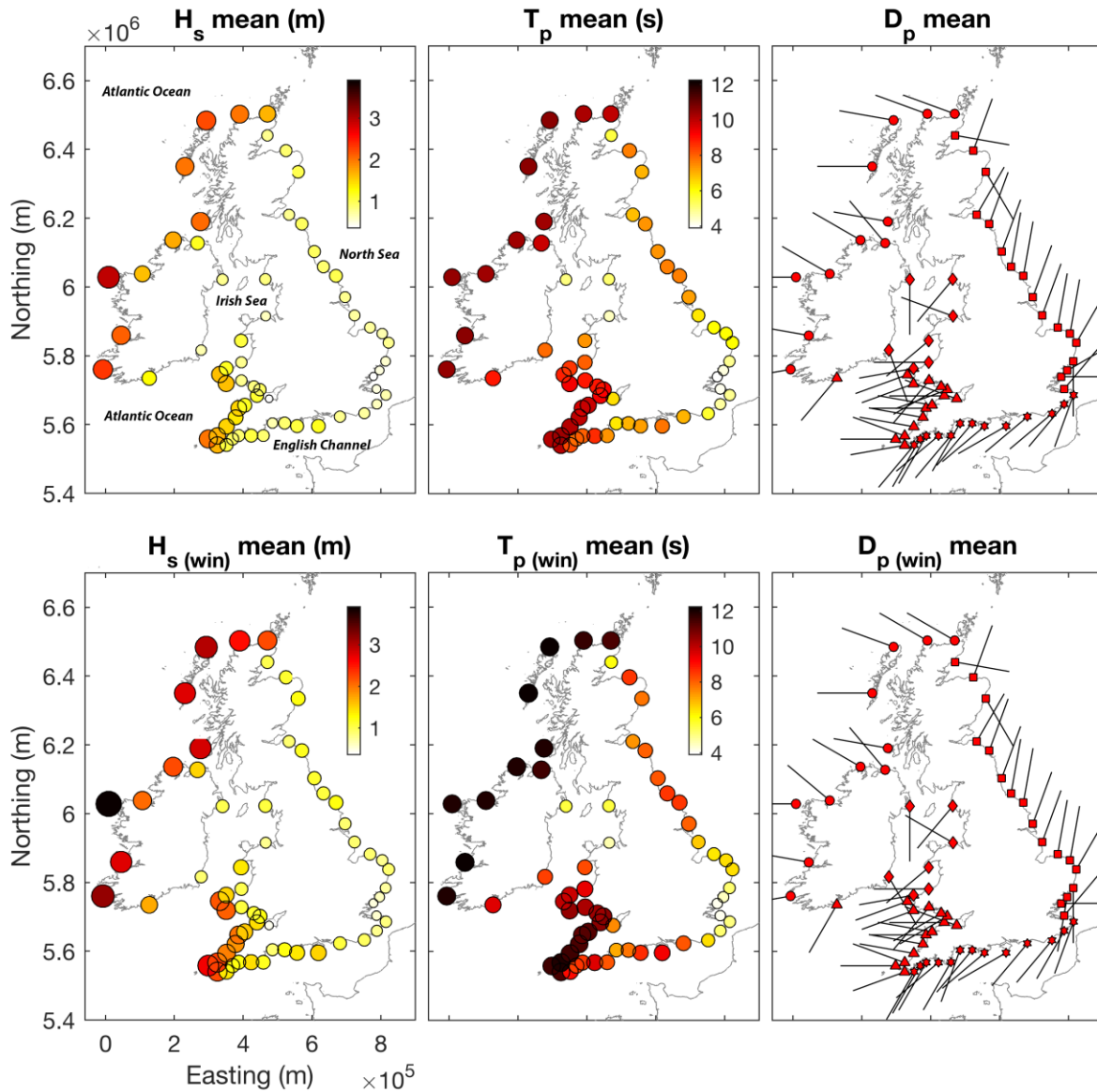


Figure 1. Overview of annual (top panels) and winter (bottom panels) wave climate (1980–2017) around the UK&I coast (all 63 wave model nodes) – mean significant wave height (left panels), mean peak wave period (middle panels), modal peak wave direction (frequency of occurrence; right panels). The size of symbols (left/middle) are proportional to colormap values.

between Valentia (Ireland) and Santa Cruz de Tenerife (Canary Islands). Although the WEPA contains some variability of EOF-based NAO, EA, EA/WR and SCAND, it was used as it provides a simple SLP-based index that best explains winter wave height variability along the coast of western Europe, from UK to Portugal (52–36°N), and which reflects a latitudinal shift of the Icelandic low / Azores high dipole. We also used the Arctic Oscillation (AO), a climate index

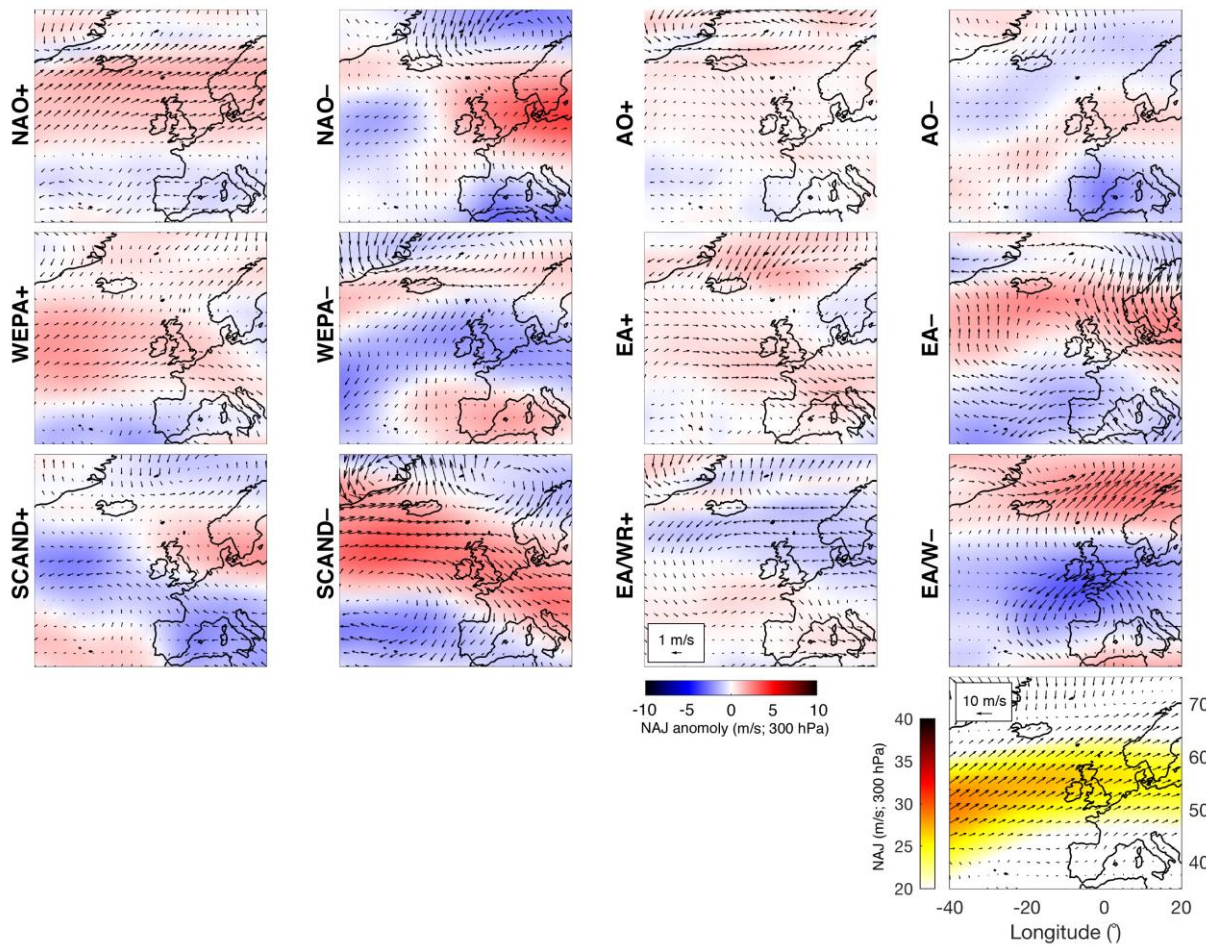


Figure 2. Atmospheric signature of all indices used in this study. Panels show sea surface wind (vectors) and 300 hPa winds relating to the North Atlantic Jet (NAJ; red/blue colours) anomalies from long term mean. Positive phase and negative phase of each index is addressed by averaging the 5 years with the largest and smallest index values over 1980–2017, respectively. Variability is displayed as anomalies from the long-term mean (1980–2017). Long-term mean sea surface wind field (vectors) and NAJ 300 hPa wind speed (colour) are shown in bottom right panel for entire period.

representing the state of the atmospheric circulation of the Arctic computed by projecting the AO loading pattern to the daily 1000-mb height field anomaly above 20°N. The loading pattern of the AO is the leading mode from EOF analysis of monthly mean 1000-mb height for 1979–2000. While research has debated the usefulness of the AO, suggesting it is expressing the same physical phenomenon as the NAO (Itoh, 2008), it is included in this study due to the potential insights it may provide for subtle changes in directional wind-wave fields in sheltered seas. These regional atmospheric signatures are highlighted in Figure 2, illustrating the association of +NAO and -SCAND with increased westerly winds at high latitudes, and -NAO and +SCAND linked to reduction in westerly airflow and blocking of the North Atlantic Jet (NAJ). It is also clear from Figure 2 that +WEPA represents a southward shift and strengthening of westerly sea surface winds in North Atlantic.

Season-ahead retrospective forecasts (hindcasts) of the winter-averaged December–March (DJFM) NAO and WEPA are provided by version 3 of the Decadal Prediction System (DePreSys3) of the UK Met Office, as outlined in Dunstone et al. (2016). Forecasts were run for winters over the period 1980–2016, with hindcasts initialized on 1st November each year. The NAO is calculated using the Azores–Iceland definition (similar to that used in Dunstone et al. (2016), but now for DJFM (December–March). There is a significant correlation skill score for the season-ahead forecasts of the observed pressure-dipole based NAO $r = 0.57$ ($p < 0.05$). WEPA is calculated using the Canaries–Ireland definition (similar to that used in Castelle et al. 2017) but there is poor correlation skill score for the season-ahead forecasts of observed pressure-dipole based WEPA ($r = 0.13$, $p \gg 0.05$).

Atmospheric data were derived from the National Centers for Environmental Prediction (NCEP)/ National Center for Atmospheric Research (NCAR) Reanalysis 1 project (downloaded from www.esrl.noaa.gov/psd/data/gridded/data.ncep.reanalysis.html), providing gridded ($0.25^\circ \times 0.25^\circ$) 4 times daily (0Z, 6Z, 12Z, and 18Z) vector winds at 17 pressure levels from 1948 to the present (Kalnay et al., 1996).

3. Wave climates in the UK and Ireland

Figure 1 provides an overview of the 63 inshore wave data nodes that span all the sheltered and exposed regions of the UK&I. These regions can be qualitatively separated into their geographic regions based on their wave exposure (annual/winter mean wave climate) and the characteristics of the directional modality of the wave climate (Table 1; Figure 3). Integrated winter wave climate is composed of months December through to March (DJMF), following previous analysis of climate indices (e.g., Castelle et al., 2017). To assess directional multi-modality throughout the UK&I and investigate the explanatory power that climate indices may have on the directional balance of alongshore wave power at these inshore locations, directional modes were extracted from the cumulative directional wave power distribution for each wave node around the coast and ordered by energy peak for 1980–2017 (Figure 3; right). Analysis of direction modality shows that 46 of the nodes (73%) have directionally multimodal wave climates where secondary modes ($> 5\%$ of primary mode peak prominence) have $> 20^\circ$ peak-to-peak separation. Across all nodes, mean prominent peak half power width = 22° ; therefore, it can be estimated that $> 70\%$ ($\sim 2.35\sigma$) of peak distribution is within 20° of peak.

In general, the most exposed west coast regions (winter-averaged significant wave height $H_s > 1.5$ m and peak wave period $T_p > 9$ s; W Ireland and SW England & Wales) display the lowest levels of directional multimodality (20% and 33% of nodes, respectively) with NW Scotland being the exception (60%) due to a broad ocean swell window (Table 1; Figure 1). All nodes along the coasts of S & E England throughout the English Channel and North Sea coasts are directionally multimodal; these regions are also the most sheltered from open ocean swell and are the only regions where winter $H_s < 1.2$ m. Moving up the North Sea coast into NE Scotland, there is an increasing influence of northerly swell waves from the Arctic (winter $T_p = 7.4$ s), but wave climate bi-directionality still dominates (100% of nodes) until the north-facing coast of NW Scotland is reached. Coasts of W Wales, NW Wales & NW England, and E Ireland are located within the Irish Sea with varying influence of S-SW Atlantic swell waves, resulting in much of the region being dominated by local wind wave regimes and local influence of coastal orientation (winter $H_s = 0.9$ – 1.3 m and $T_p = 5.1$ – 9.4 s; Table 1).

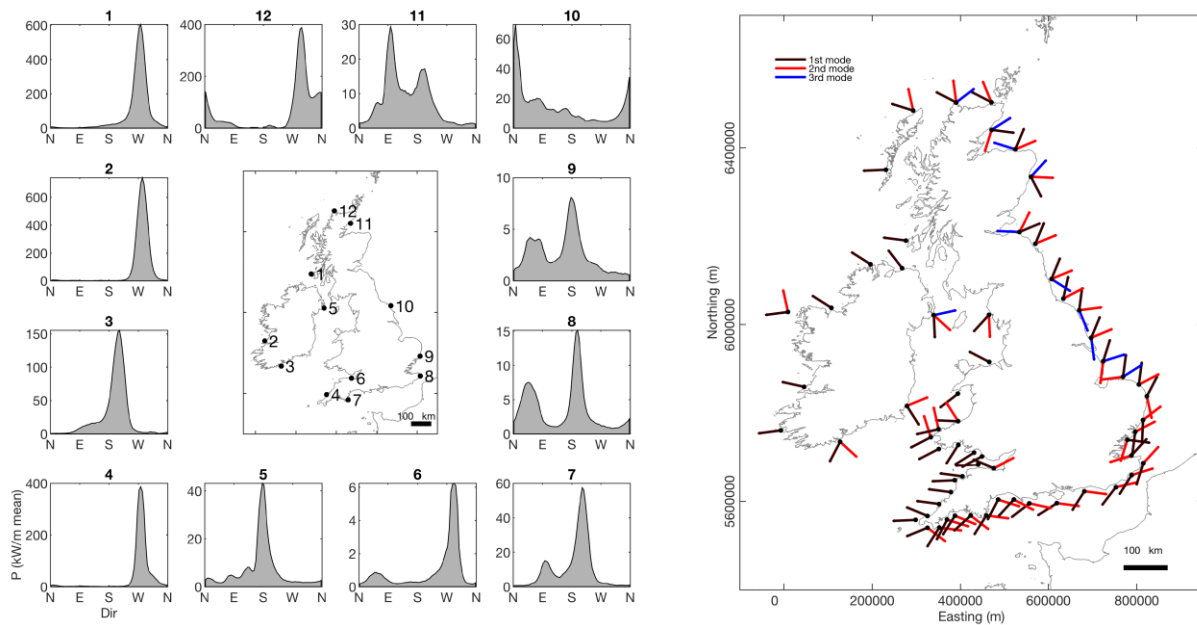


Figure 3. Left: Regional examples of winter (DJFM) wave climate data showing distribution of directional wave power (cumulative). Insets are 3-hourly average kW/m in 5° bins for 1980–2017. Right: Quiver plot shows dominant directional modes (1980–2017) from cumulative wave power distribution for all coastal nodes. Black, red and blue are primary, secondary and tertiary, respectively. Modes displayed are > 5% of primary mode peak prominence.

Table 1. UK hindcast wave climate statistics for the period 1980–2016. Nodes shown in Figure 1 are integrated into regions of similar characteristics and exposure. Winter wave statistics represent months Dec–Mar.

<i>Region</i>	<i>Nodes(n)</i>	<i>Annual H_s (m)</i>	<i>Annual T_p (s)</i>	<i>Winter H_s (m)</i>	<i>Winter T_p (s)</i>	<i>Bi-directionality (%)</i>
NW Scotland	5	2.0	10.3	2.7	11.8	60
W Ireland	6	2.0	10.3	2.6	11.9	20
SW England & Wales	12	1.3	9.4	1.7	10.8	33
W Wales	4	1.2	8.2	1.5	9.4	75
E Ireland	4	1.0	7.9	1.3	8.7	75
S England	13	0.9	6.7	1.1	7.5	100
NE Scotland	3	0.9	6.7	1.1	7.4	100
NW Wales & NW England	2	0.7	4.8	0.9	5.1	50
E England	14	0.7	6.1	0.9	6.6	100

Initial wave climate analysis indicates that beyond the semi-sheltered sites examined in Wiggins et al. (2019) along the western English Channel coast, directionally bimodal wave climates exist in many inshore regions throughout the coasts of the UK&I. Of particular interest are nodes along the English Channel coast (S England) and southern North Sea coast (E England) where primary and secondary directional modes are from opposing directions with respect to the coastal shore-normal, therefore having the greatest potential to influence coastal morphodynamics and shoreline plan-shape rotation with respect to the directional balance of alongshore wave power (Figure 3).

4. Role of atmospheric indices

The associations between long-term atmospheric forcing and wave climate, for inshore waters of UK&I, were investigated by correlating the winter-averaged climate indices (NAO, WEPA, SCAND, AO, EA and WR/EA) with total winter-averaged wave power (1980-2017), for nodes in Figure 4. All references herein to climate indices are DJFM winter averaged. Total winter-averaged wave power was found to be significantly correlated with NAO for Atlantic NW coasts ($r = 0.6-0.83$; $p < 0.05$), consistent with earlier findings (Martínez-Asensio et al., 2016; Castelle et al., 2017). Correlations for the Atlantic SW and within the Irish Sea were also significant, though with lower coefficients ($r = 0.39-0.58$; Figure 4). Similar spatial relationships occur for the AO, though limited to the west Atlantic, and with lower coefficients ($r = 0.5-0.8$, Atlantic NW; $r = 0.31-0.4$, Atlantic SW). As previously determined (Castelle et al., 2017), the NAO has limited skill in predicting total wave power south of southern Ireland ($\sim 52^\circ\text{N}$), with WEPA and EA displaying a corresponding increase in skill in this region. WEPA and EA only show positive correlations with wave power for the southern half of UK&I, with WEPA outperforming EA (15% greater explanation of variance, where significant correlations exist). WEPA has the greatest predictive skill in the southwest ($r = 0.66-0.79$, Atlantic SW coast; $r = 0.81-0.84$, W English Channel). Wave power along the Atlantic NW exposed coast are also correlated with negative SCAND ($r = -0.32$ to -0.63), while the semi-sheltered North Scotland coast is correlated with positive SCAND ($r = 0.21-0.6$). The significance map of SCAND is broadly an inverse of the AO.

In the context of previous ocean basin-scale research, significant positive relationships with the NAO, AO, WEPA and EA, and also negative SCAND, for total wave power on Atlantic coasts were expected, but inshore regional scale (including shelter seas) analysis here reveals significant negative correlations with NAO/AO and positive correlations with SCAND along the mixed swell/wind-wave dominated east-facing North Sea coast (NAO $r = -0.28 - -0.69$; AO $r = -0.41 - -0.71$, SCAND $r = 0.33 - 0.65$) with AO showing the strongest relationship and level of significance (all sites significantly correlated at 95% level). This analysis shows that the EA/WR index provides the least explanatory power of all the indices tested.

The associations between wave direction and climate were further explored by correlating the climate indices with cumulative directional winter wave power, within an angular window spanning $\pm 20^\circ$ of the modal peak (Figure 5). Results show a striking degree of correlation across multiple indices (NAO, AO, WEPA, EA, SCAND), with strong contrasts between indices. This indicates that a significant amount of winter-wave directional variability within UK&I can be explained by variations in climatic modes, with correlations apparent even for some sheltered wind-wave dominated regions away from Atlantic swell.

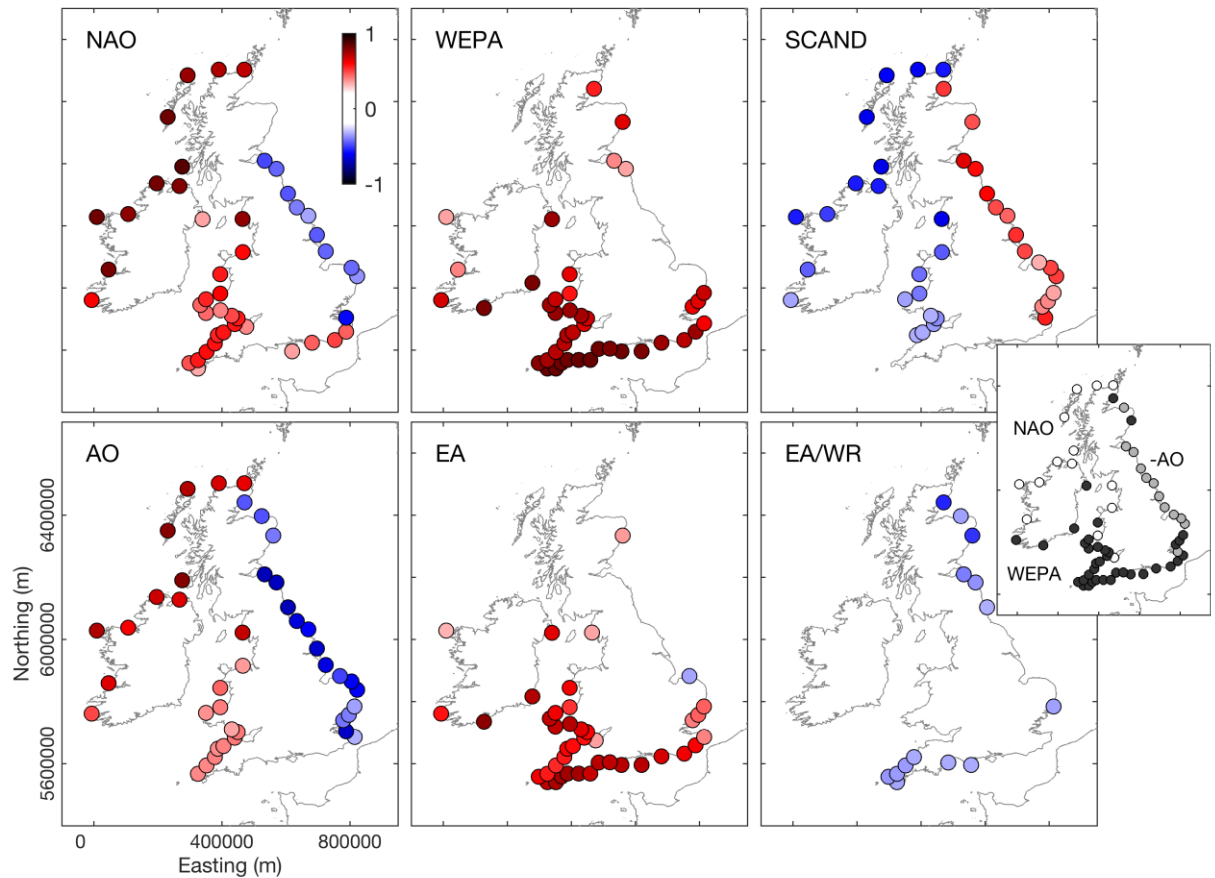


Figure 4. Correlations between mean winter wave power and six winter-averaged atmospheric indices (NAO, WEPA, SCAND, AO, EA and EA/WR) for 63 locations around the coast of the UK&I. Only locations where correlation coefficients (r) were significant at 95% level are shown ($p < 0.05$). Inset shows leading explanatory index for each node (white = NAO, black = WEPA, grey = AO).

All nodes in the southern Ireland, English Channel and southern North Sea coasts (south-facing) are strongly directionally bimodal (Figure 3), with coastal orientation suggesting dominance of alongshore sediment transport processes, which is supported by observations along this coast by Wiggins et al. (2019b). Analysis shows that WEPA (and EA to a lesser extent) significantly explains variability in winter-averaged wave power for all southwesterly orientated (principal) wave directional modes ($r = 0.58-0.77$), accounting for the largest proportion of winter-averaged wave power. In contrast, negative NAO explains variability in all easterly-orientated wave modes ($r = -0.6 - -0.76$), with positive SCAND also contributing high correlations with easterly waves ($r = -0.5 - -0.67$). These findings mean the full winter-averaged directional wave power balance is significantly explained by climate indices along this whole section of coast.

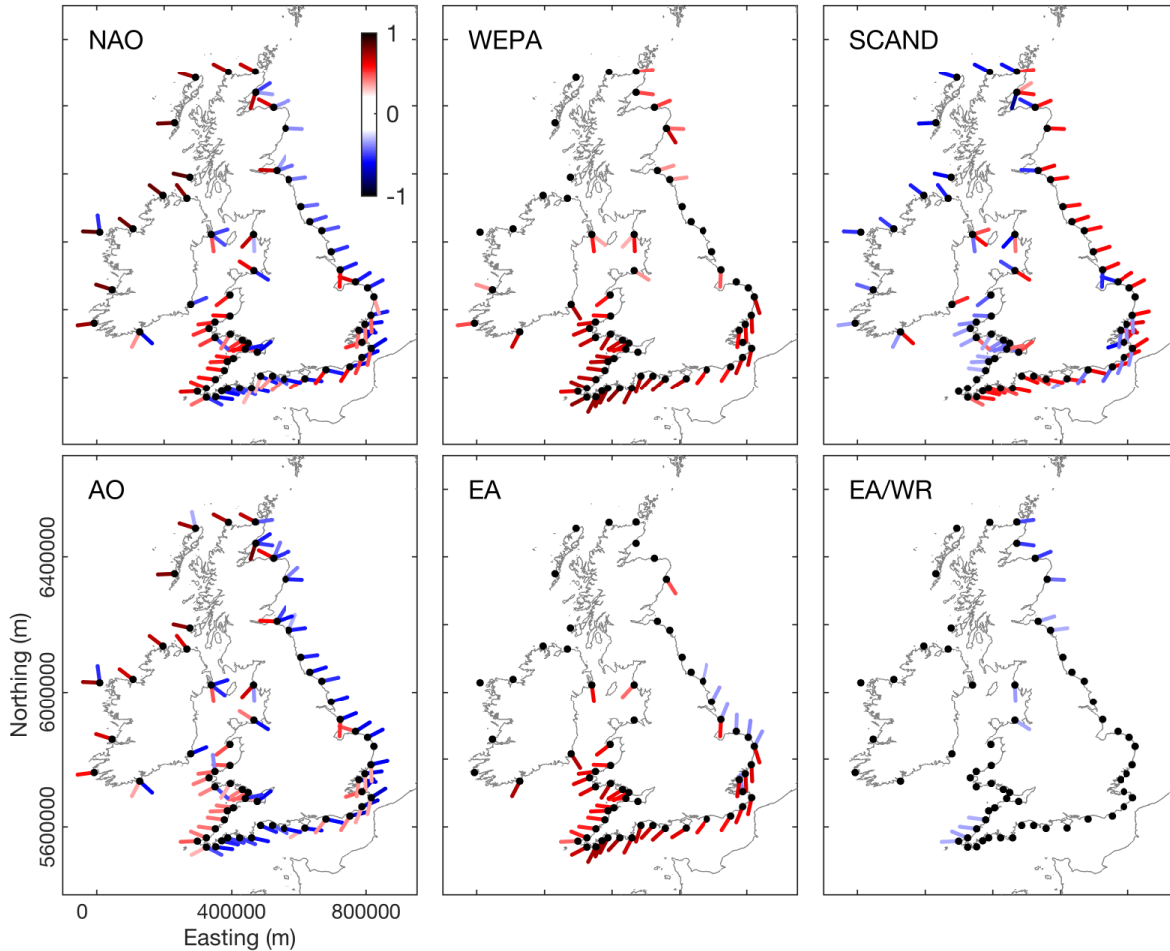


Figure 5. Relationship between winter-averaged NAO, WEPA, SCAND, AO, EA and EA/WR and directional winter-averaged wave power (local wave directional window of $\pm 20^\circ$ for each node) for 63 wave nodes (black dots) around the coast of the UK&I (1980–2017). Colors are correlation coefficients (r), only results where $P < 0.05$ are shown.

Beyond the south coast regions, easterly-orientated wave modes throughout the bi-directional North Sea region, characterized by short wind-waves, showed significant relationships with negative NAO (and AO) where $r = -0.35 - -0.57$ ($r = -0.5 - -0.62$) decreasing to the north. The strongest relationships in the North Sea region are found with the SCAND index, showing significant positive correlations with all easterly-orientated nodes where $r = 0.57-0.62$. Interestingly, EA and AO, and NAO to a lesser extent, had some skill in explaining northerly swell waves entering this North Sea region, but only regionally. This northerly component is an important element of the northern North Sea coastal wave climate and is associated with a small swell window and is strongly impacted by coastal orientation. Whilst EA provided some skill in explaining northerly wave mode variability at six southern North Sea coast sites, significant r -values only reached 0.39. AO and NAO showed some explanatory power for six nodes in the northern North Sea regions (E. Scotland) with significant r -values between 0.33 and 0.59 (Figure 5).

Throughout the UK&I there are sheltered regions with complex coastal orientations (e.g., E Scotland, Irish Sea and Bristol Channel) sheltered from significant swell-wave contribution and that are dominated by a locally generated wind-wave climate. The directional wave modes in these regions display a variety of significant relationships with indices dependent of spatial location and coastal orientation. Typically, easterly-oriented short fetch nodes are related to negative NAO/AO, and positive SCAND; whereas westerly-oriented short fetch nodes are related to positive NAO/AO, and negative SCAND.

In summary, winter-averaged climate indices show strong and significant correlations with directional winter-averaged wave power throughout the UK&I. Analysis indicates there are regionally-coherent relationships between directional waves and various combinations of the leading climate indices. To examine the temporal variability and predictability of regional response characteristics, a quantitative connectivity-based cluster analysis is first undertaken.

5. Characterization of regional response

Regionally-coherent relationships between the climate indices shown to provide the most explanatory power in determining directional wave variability in UK&I were investigated through hierarchical cluster analysis. For all 63 nodes, the variables examined were mean directional winter wave power correlation coefficients with NAO, WEPA, AO, SCAND and EA for the period 1980–2017. EA/WR was excluded at this stage as spatial correlations were weak and mostly statistically insignificant. EA and AO were retained as they provided some explanatory skill for northerly waves in the North Sea. The clustering uses Euclidian-based proximity to determine similarity between nodes where response variables are primary and potentially secondary directional mode correlations with winter-averaged climate indices. The dendrogram shown in Figure 6 shows the results of the cluster analysis where Ward's minimum variance method is used to minimize the total within-cluster variance (weighted squared distance between cluster centers) at each step (Ward 1963). The advantage of Ward's method is that it often provides a clear threshold number of groups where there is a large jump in group merging cost (e.g., above and below similarity level 1; Figure 6).

Four clear groupings were defined by this classification process (Figure 6). Two groups named South West and North West clearly represent the largely directionally uni-modal west coasts that are dominated by ocean swell waves. A group named South represents nodes that are bi-directional in nature and largely located on the southern and western regions of the UK&I. The final major group named East also represents bi-directional wave climates, but the region is limited to the eastern North Sea coast and only consists of sites exposed to northerly swell waves. To elucidate the driving climate control relationships of each group, example nodes (A-E; Figure 6) representing case study sites from each cluster, were examined further.

Figure 7 examines the atmospheric indices controlling the wave climate at each case study site. Where the wave climate is directionally uni-modal, the standardized long-term (1980–2017) winter-mean wave power timeseries is examined through a wave power index (P_{index}). Where the wave climate is significantly directionally bimodal, a wave power directionality index (WDI) is computed following Wiggins et al. (2019a), which represents the winter-averaged standardized wave power balance between two opposing wave directional modes, shown by Wiggins et al. (2019b) to correlate with observed beach rotation. At each node, an index of the

relative balance between winter wave power contributions from the two modal directions is computed, using the equation:

$$WDI = \frac{(P_1 - P_2) - \overline{(P_1 - P_2)}}{\sigma(P_1 - P_2)} \quad (1)$$

where $(P_1 - P_2)$ is the residual wave power between the first (prominent) and second directional wave power modes, $\overline{(P_1 - P_2)}$ is the long-term mean and $\sigma(P_1 - P_2)$ is the long-term standard deviation of that difference. High positive values of WDI indicate that the primary directional mode is more prevalent than the long-term average, whereas high negative values indicate that the wave climate has a higher proportion of the secondary directional mode than average.

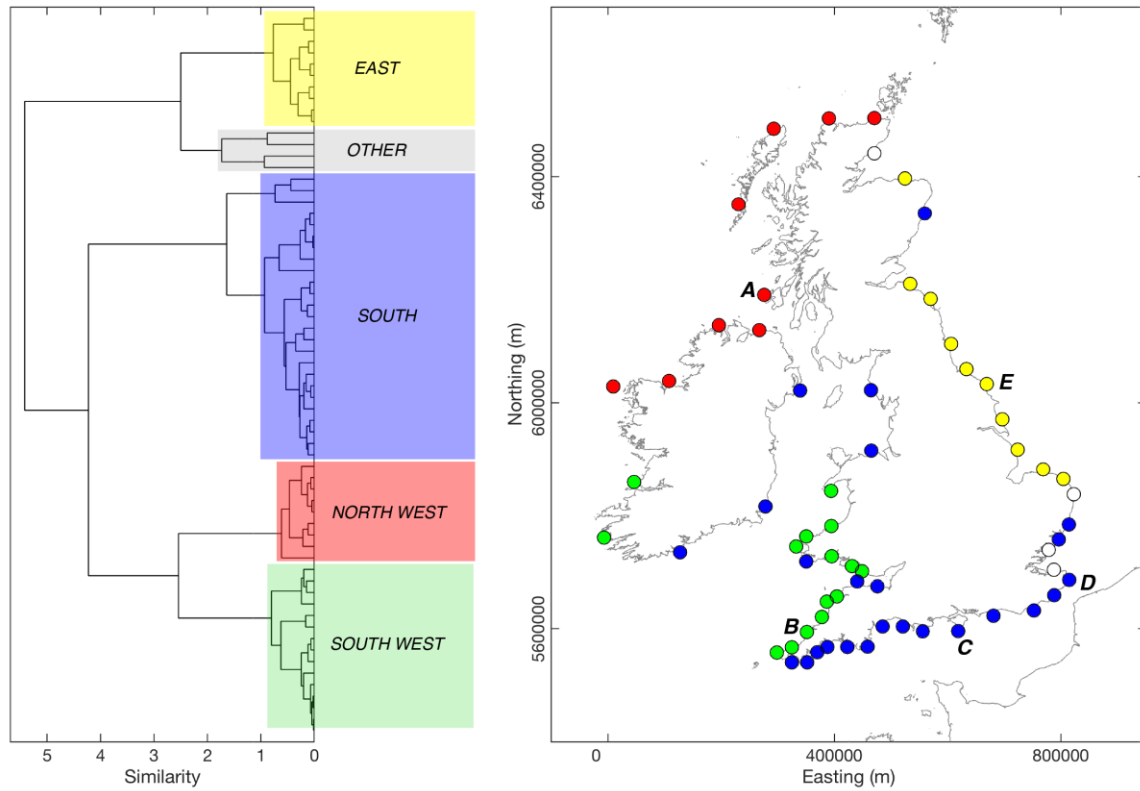


Figure 6. Regional classification of correlations between winter-averaged directional wave climate response (mean wave power for dominant directional modes) and most significant winter-average atmospheric indices NAO (EOF-based), WEPA (station-based), and SCAND (EOF-based) for the period 1980–2017. Left: Dendrogram illustrating results of hierarchical agglomerative cluster analysis, using Ward’s minimal increase of sum-of-squares Euclidian proximity method. Clear groupings are labelled. Right: Groupings from cluster analysis presented spatially, with nodes A-E representing case-study sites from each region used for further analysis and visualization.

For all bi-directional example sites shown in Figure 7, WDI time-series show significant temporal variability over the 37-year period. WDI within the South region (sites C and D; Figure 7 left panel) displays a consistent 5–8 year cyclicity that can be observed from the continuous wavelet transform analysis shown in Figure 7 (right panels) computed as in Castelle et al. (2018) using a scaled and normalized Morlet function, following Grinsted et al. (2004). Periodicity is strongest and most significant since 2005. This corresponds to the periodicity observed in the WEPA index by Castelle et al. (2018) through similar wavelet analysis. WDI at these South group sites is significantly positively correlated with WEPA, NAO and SCAND, with WEPA having a stronger correlation in the west of the region (site C) and NAO/SCAND increasing in importance the east (site D). The case study site from the East group in the mid North Sea coast (site E) shows a significant 5–6 year periodicity in WDI, but with limited negative phases between 2000–2010 and shows weak or insignificant correlations to the climatic indices tested, with the exception of SCAND. As has already been shown, example sites from North West and South West groups, which are directionally uni-modal, P_{index} are strongly correlated with NAO and WEPA, respectively, and are therefore dominated by any periodicity of these indices. Unlike WEPA, there is little coherent periodicity displayed within NAO dominated sites (site A) and there are high degrees of variability over the period 1980–2017, with the only significant timescales of ~2 years occurring post 2010 (Figure 7a-b; right panel). This lack of NAO periodicity has previously been demonstrated by Barbosa et al. (2006) and Castelle et al. (2018).

It is clear that the inter-annual variability of winter-averaged directional wave power throughout the UK&I is well explained by a range of individual indices, but it is useful to explore whether or not when combined they have greater predictive skill, particularly for bi-directional regions. Empirical stepwise multiple linear regression models were computed for each example site using combinations of the leading indices for each location based on correlation analysis and their predictive skill is presented in Figure 7 (left panels). For all sites, except site A in the North West group, the combination of multiple indices in a linear model outperformed the use of a single index. The model elements are presented in Table 2. Both sites from exposed uni-directional groups (North West and South West) demonstrated very skillful reconstructions of winter wave power with combinations of NAO and WEPA with r -squared values exceeding 0.75. Specifically, site B from the South West group demonstrated the improved skill gained by utilizing the product of two indices (r -squared = 0.8). WDI from the South group (sites C and D) was skillfully predicted utilizing a combination of NAO, WEPA and SCAND. The discriminatory power of these combined indices is visualized in NAO/WEPA and NAO/SCAND parameter space (Figure 7; middle panels) demonstrating, for example, that at site C all winters experiencing positive WDI occurred when both NAO and WEPA were positive. Likewise, SCAND when combined with EA at site D accounts for a greater proportion of the variance in WDI. Finally, in the East region (site E), where SCAND was the only index significantly correlated with WDI ($r = 0.35$), the combination of NAO, WEPA and SCAND with EA generated a linear model with significant explanatory skill (r -squared = 0.45), where the combination of SCAND and EA at site D go some way in discriminating between WDI+ (dominance of waves from the northerly mode; EA–) and WDI– (waves from the easterly mode; +SCAND).

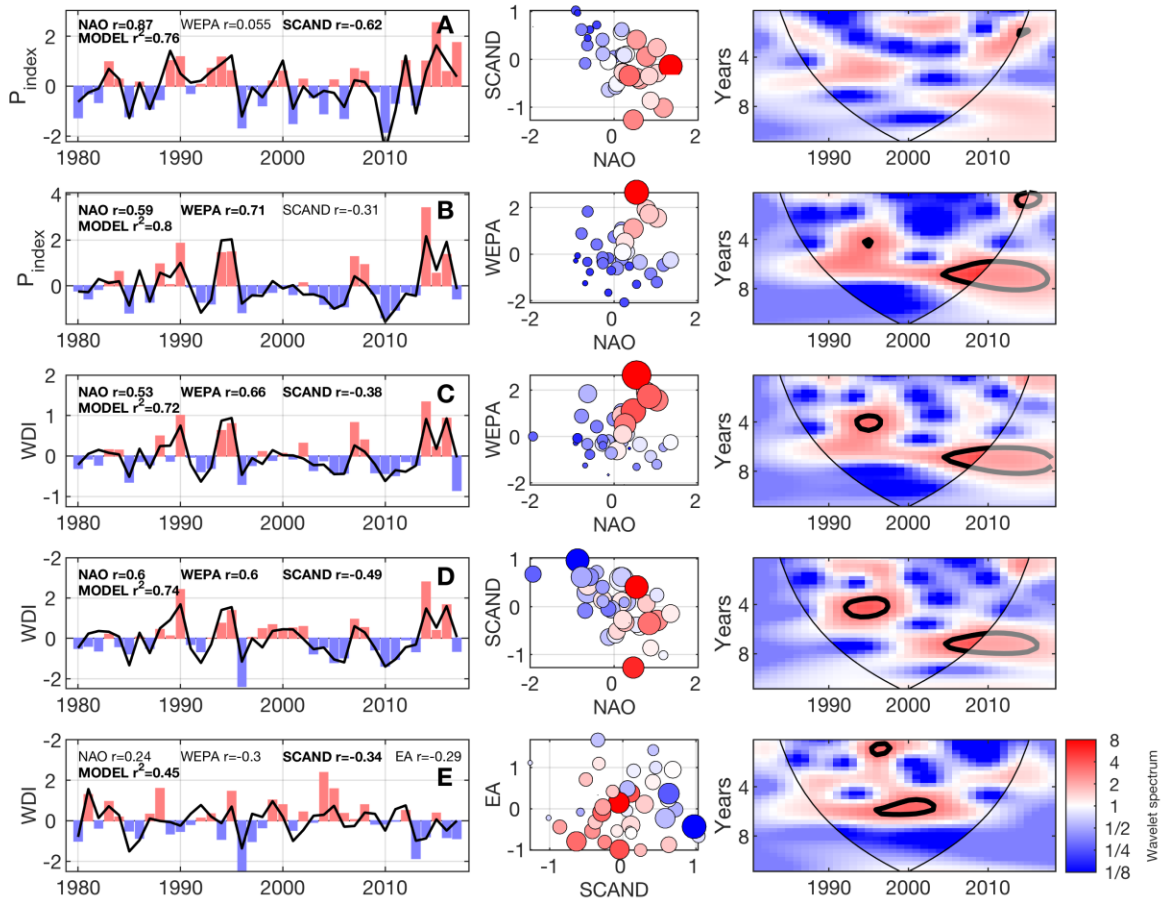


Figure 7. Temporal variability of standardized winter-averaged wave power (P_{index} ; uni-directional regions) and wave direction (WDI; bi-directional regions) for case study sites from each of the 4 major classified regions are shown. Locations of sites A-E are shown on Figure 6. Left panels show 1980-2017 wave power (P_{index} ; top two panels A-B) and winter-averaged WDI timeseries (bottom three panels C-E) for each winter season as red/blue bars, for each site correlations (r) with winter-averaged NAO, WEPA and SCAND are shown (bold is significant at the 95% level). In addition, stepwise multiple linear regression (SMLR) model r -squared values are shown (bold is significant at the 95% level) and model prediction line is shown (bold black). Middle panels show winter-averaged P_{index} (top two) and WDI values (bottom three) within a 2D parameter space of the leading explanatory variables from SMLR for each site. Color is P_{index} or WDI (low/high = blue/red, white = zero), bubble size is standardized winter wave power. Right panel shows local wavelet spectrum normalized by the variance of associated power and wave direction index. In wavelet panels, the 5% significance level against red noise is contoured in bold black line and the cone of influence is delimited by the fine black line.

389

390

The atmospheric expression of modelled P_{index} and WDI values from case study sites for each classified region (1980–2017) are explored in Figure 8 by taking the highest and lowest 5 years for each P_{index} (the same methodology as Figure 2). The highest five P_{index} years ($P+$) at North West and South West example sites (site A and site B) reflect the atmospheric signature NAO+ and WEPA+, respectively (Figure 2). In both sites (in particular site B), the influence of the positive and negative SCAND patterns can be seen in both surface winds and the NAJ anomaly. The $P+$ anomaly seen in the North West group case (site A) is expressed as an increase in northwesterly surface winds above 55°N and a northward shift of the NAJ, while in the South West group case (site B) $P+$ corresponds to a clockwise rotation of the NAJ with a striking southward dip below 50°N over UK&I and NW Europe; this NAJ southerly shift is somewhat characteristic of WEPA+ and SCAND-. Certainly, the most significant difference in $P+$ between the North West and South West group cases is the increase in westerly surface winds below 53°N (southern Ireland) for the latter when compared to a NAO+ ($P+$ site A) scenario. This observed relationship between the NAJ and NAO is unsurprising and as year-to-year variability in the NAO is known to describe the state of the Atlantic jet stream which is directly related to near-surface winds across North America, Europe, and other regions around the Atlantic Basin (Scaife et al. 2014). For the bi-directional South group (site C), the WDI+ expression is strongly reflected in WEPA+ with increased westerly surface winds over the southern half of the UK&I. The WDI- expression is one of increased southeasterly anomalies in surface winds throughout the English Channel and North Sea and a dramatic reduction in westerly winds in the North Atlantic, limiting southwesterly swell in this region; this is associated with an Atlantic shift of the NAJ to the north ($>65^{\circ}\text{N}$) or south ($<45^{\circ}\text{N}$) away from the western approaches and reflects patterns of SCAND+ and NAO-. The WDI+ atmospheric expression from the East group (site E) shows a very strong latitudinal shift of the NAJ below 50°N represented by a reduction in NAJ windspeeds of $\sim 5 \text{ ms}^{-1}$ throughout the north and increase to the south. A strong northeast surface wind anomaly ($> 2 \text{ ms}^{-1}$) above 50°N throughout the North Sea and NE Atlantic represents a condition that may be representative of increased northerly swell wave propagation into the North Sea. This pattern is not clearly reflected in NAO, WEPA or SCAND, but can be partially reflected in the EA- pattern (Figure 2). The signature of WDI- in the East group is even less clear reflecting the complexity of the wave climate and highlight issues/limitations of trying to use climate indices to predict directional wave climate in this region (East).

6. Discussion and conclusions

This study has shown there exists strong and significant connections between leading climate indices in the North Atlantic and winter-averaged wave power in inshore regions, both in exposed and (semi)- sheltered coastlines. For the first time, we have demonstrated the full extent of directionally bimodal inshore wave climates around the coast of the UK&I, as well as the significant role climate indices play in explaining their inter-annual variability over four decades. It is well established that climate indices like ENSO in the Pacific and AO/NAO in the Atlantic are leading modes of atmospheric variability and strongly affect winter wave energy (Dodet et al., 2010; Bromirski et al., 2013; Castelle et al., 2017), and recent studies have also shown how extreme phases can lead to large-scale coastal erosion and shoreline change (Masselink et al., 2016; Barnard et al., 2017; Dodet et al., 2018). But, there is now a growing base of evidence highlighting the role leading modes of climate variability also have in controlling wave direction and associated longshore sediment re-distribution and shoreline rotation at the coast (e.g., Silva et al., 2012; Splinter et al., 2014; Goodwin et al., 2016; Wiggins et al., 2019b). In extreme cases,

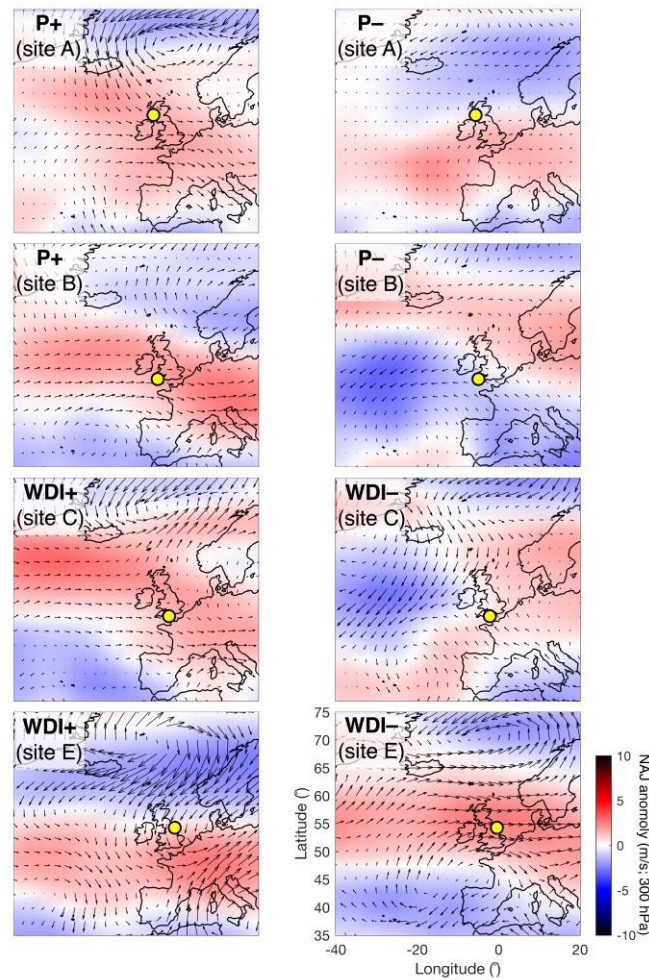


Figure 8. Atmospheric expressions of the directional wave power indices (P_{index} and WDI) for example sites (yellow circles; A, B, C, and E) in each response group (North West, South West, South and East; top to bottom). Methodology and symbology as per Figure 2.

Table 2. Stepwise multiple linear regression models for winter-mean wave power (sites A and B) and WDI (sites C, D and E) as a function of combined climate indices. Coefficients are standardized weightings of significant variables used in the model.

Site	Index	Weight	RMSE	r^2	p-value
A (NorthWest)	NAO	1.29	0.50	0.76	2×10^{-12}
B (SouthWest)	NAO*WEPA	0.32	0.46	0.8	4×10^{-12}
C (South)	NAO*WEPA	0.33	0.56	0.72	9×10^{-9}
	SCAND	-0.49			
D (South)	NAO	0.47	0.54	0.73	2×10^{-9}
	WEPA	0.59			
	SCAND	-0.68			
E (East)	NAO* SCAND	0.74	0.82	0.45	25×10^{-3}
	WEPA* SCAND	-1.18			
	SCAND*EA	1.47			

as shown by Wiggins et al. (2019a) when studying the impacts of the extreme storm wave events of the 2013/14 winter in Northwest Europe, resultant embayment rotation in semi-sheltered regions can lead to extreme coastal vulnerability and infrastructural failure.

These relationships between climate variability and inshore directional wave forcing are critical for our understanding of multi-annual and multi-decadal coastal dynamics. The analysis of 37 years of hindcast wave data from 63 inshore nodes around the entire coast of UK&I has shown that 73% of studied sites have directionally bimodal wave climates (where secondary modes are > 5% of primary mode peak prominence), with all sites within the English Channel and North Sea regions found to be directionally bimodal. Of specific relevance to coastal dynamics, primary and secondary modes within the English Channel and the southern North Sea coasts are opposing with respect to the coastal normal and have the greatest potential to influence coastal morphodynamics due to the importance of the directional balance of alongshore wave power. This is evidenced by Wiggins et al. (2019) through the examination of a decade of beach observations and embayment rotation along the south coast of England. Importantly, the analysis of these wave directional modes as a function of leading climatic indices found that combinations of the NAO, WEPA, SCAND and EA significantly explained the directional variability in winter-averaged directional wave power throughout all coasts and modal directions within the UK&I.

The seasonal variability of directional winter wave power throughout the UK&I also demonstrated clear regional coherence. Cluster analysis of all coastal nodes driven by winter-averaged directional wave correlations with NAO, WEPA, SCAND, AO and EA for the period 1980–2017 identified four key regions that had distinct responses to atmospheric variability. The classes were strongly defined by wave exposure, coastal orientation and latitude; and the regional classes were closely related to the impact that sea surface and NAJ wind expressions of related indices could have on directional waves. Empirical multiple linear regression for regional examples from each class demonstrated significant skill ($r^2 = 0.5\text{--}0.8$) for both uni- and bi-directional sites, where skill in bi-directional sites was significantly improved through the combination of multiple indices when variability of contrasting directional modes was explained by different indices. Similar observations were made by Woollings et al. (2010) who had some success in explaining the location and strength of the NAJ with a statistical mixture model defined by the NAO and the EA (similar to WEPA).

The relation between large scale seasonal atmospheric behavior and wave directionality along both exposed and more sheltered coasts that are dominated by longshore sediment transport processes is important to enable development of skillful long range forecasting of coastal dynamics. A similar approach has seen some success in seasonal forecasts of precipitation in the UK (Baker et al., 2018). These relationships can also facilitate the extension of our understanding of past (historic) coastal behavior, due to the fact atmospheric sea level pressure (and proxy) records (e.g. Luterbacher et al., 1999; Camus et al., 2014) and modelled wave re-analysis' (e.g. Santo et al., 2015), whilst containing inherent uncertainties, are much longer than those of sea surface waves or coastal morphological observations (<40 years; e.g., Turner et al., 2016). The extent of variability and periodicity of each of the leading atmospheric indices provides insights into coastal geomorphological response of beaches past and present (e.g., Castelle et al., 2018). As shown recently by Dodet et al. (2019), coastal (beach/dune) response to the disturbance of extreme winters can be multi-annual and the rate and extent of beach recovery

is critically related to subsequent winter wave power and directionality. Therefore, an improved understanding of multi-annual to decadal variability in wave conditions and its potential prediction will be fundamental knowledge for future coastal management. In this respect, the recently launched (October 2018) French-Chinese satellite CFOSAT designed to measure simultaneously directional wave spectra and winds with innovative radar scatterometer onboard (Hauser et al., 2019), will complement the spaceborne wave spectra measurements from Synthetic Aperture Radar (Alpers et al., 1981), and allow an improved characterization of wave spectral variability at the global scale.

6.1 Season-ahead forecasting

In this context, it is useful to examine the current skill of 'season ahead' forecasts of winter-mean climate indices for explaining directional waves in the UK&I. Until recently, long-range forecast systems showed only modest skill in 'season ahead' predictions of Atlantic winter climate and the NAO, partially due to the lack of response of extratropical atmospheric circulation to long-term predictive variability of the ocean (Smith et al., 2012). However, Scaife et al. (2014) recently demonstrated significant skill ($r = 0.6$) in predicting the NAO when initialized a month before the onset of winter and argued that greater ensemble sizes would lead to greater skill (Scaife et al., 2014). One would expect from results presented in this study that wave nodes in the North West group, that were highly correlated with the NAO, would be the most forecastable. Indeed, this is borne out in Figure 9, where all uni-directional nodes between southwest Ireland and north Scotland are significantly correlated (at 95% level) with forecast NAO (1980–2016) where $r = 0.37$ – 0.52 . This relationship disappears for the South West group, where variability is more strongly linked to WEPA. Correlation scores for the bi-directional groups South and East showed significant inverse correlations (at 95% level) with secondary mode easterly waves at six sites along the English Channel coast, specifically those sites with a southeasterly orientation. At the 90% level, the easterly wave component of wave climate throughout English Channel and southern North Sea is significantly negatively correlated with forecast NAO. For sites in the South and East groups, this skill does not translate into predictability of WDI due to the strong influence of WEPA explaining the primary southwesterly directional waves. To the authors' knowledge, these findings are the first demonstration of skillful 'season ahead' forecasts for inshore directional winter wave climate and provide new evidence that medium term forecasts of coastal hazard are currently achievable for selected regions of the UK&I, and further advances in forecast skill may open the possibility for highly valuable national scale coastal vulnerability assessments.

As noted by Scaife et al. (2014), much of the forecast skill of the atmospheric model is derived from the ability to predict the NAO and this is highlighted by the lack of model skill in regions where NAO influence is weak. It is therefore unsurprising that indices explaining secondary modes of variability like WEPA are currently not well predicted ($r = 0.13$; $p = 0.353$). An examination of the skill map for predicting DJFM Mean Sea Level Pressure (MSLP, Figure 10) confirms that, on average, DePreSys3 shows little MSLP skill over UK&I (located in the region of high uncertainty due to the NAJ variability). Instead, significant skill is found to the South (over the Azores/Southern Europe) and to the North (north of Iceland and over Scandinavia). While this is a limitation for the UK&I and indices like WEPA, this does suggest that the implementation of the approach used in this study in regions of greater atmospheric model skill may yield stronger results. Encouragingly, recent studies have highlighted the

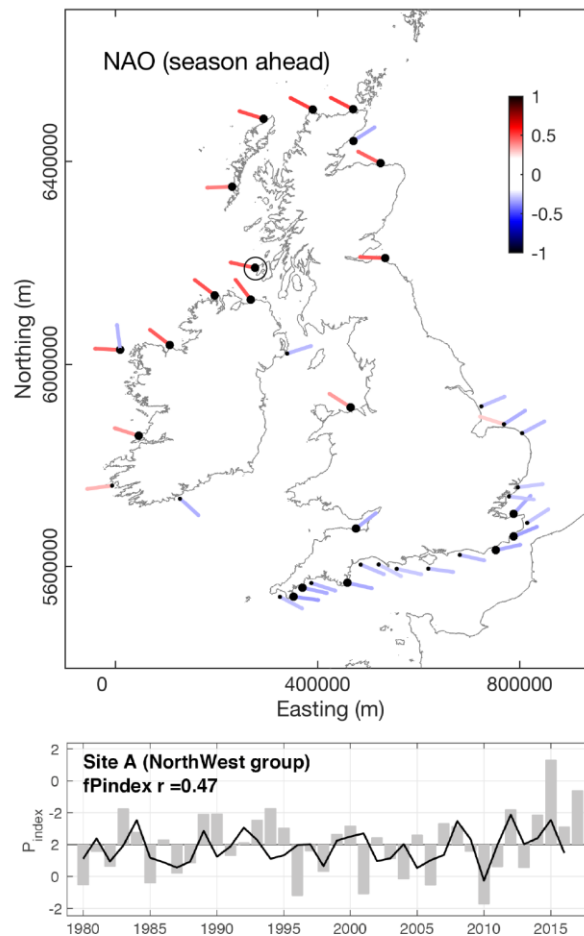


Figure 9. NAO ‘season ahead’ forecast: (upper) relationship between season-ahead forecast winter NAO and directional winter-averaged wave power (local wave directional window of $\pm 20^\circ$ for each node) for 63 wave nodes around the coast of the UK&I (1980–2016). Colors are correlation coefficients (r), only results where $P < 0.1$ are shown, larger black dots represent $P < 0.05$. (lower) Winter P_{index} timeseries for site A (NorthWest group) showing (black line) modelled P_{index} values using forecast NAO from DePrySys 3 model. Correlation coefficient is significant at 95% level.

potential for future improvements in seasonal (Athanasiadis et al., 2016) and decadal (Smith et al., 2019) forecast skill through increased ensemble sizes, citing the ‘signal to noise paradox’, which identifies that climate models (particularly for the Atlantic) are better able to predict their observed counterparts than their weak signal-to-noise ratios may suggest, meaning there may be much more potential predictability of indices like the NAO with larger ensemble sizes (Scaife and Smith, 2018). In combination with the indication that the seasonal and decadal climate may be more predictable than previously thought, the strong relationships uncovered in this study between inshore winter waves and atmospheric indices suggests that the potential for skillful long-term wave climate forecasts may be realized in the near future. This would better enable decision-makers to effectively adapt to the impact of long-term climate variability and extreme events (Smith et al., 2019).

Within the global coastal science community there is an ever-increasing focus on developing skillful long-term predictions of coastal evolution due to climate change (through increased sea-level rise and changes in storminess; e.g., Montano et al., 2020). As part of this challenge, it will be critical to account for climate variability and put observed coastal change over the past 20 years into this context. As elucidated through climate indices like the NAO, these indices can reflect natural variability in the ocean and atmosphere on inter-annual and multi-decadal scales (e.g., Scaife et al., 2014; Wang et al., 2016; McCarthy et al., 2018). Deser et al. (2017) suggested that internal variability of the NAO imparts substantial uncertainty in future changes in regional climate even out to decades ahead. This is likely overestimated due to signal to noise errors in predictions of the NAO (Eade et al 2014) but still needs to be accounted for in climate projections and predictions of directional wave climate in order to aid coastal managers to prepare and adapt to ongoing climate variability and change.

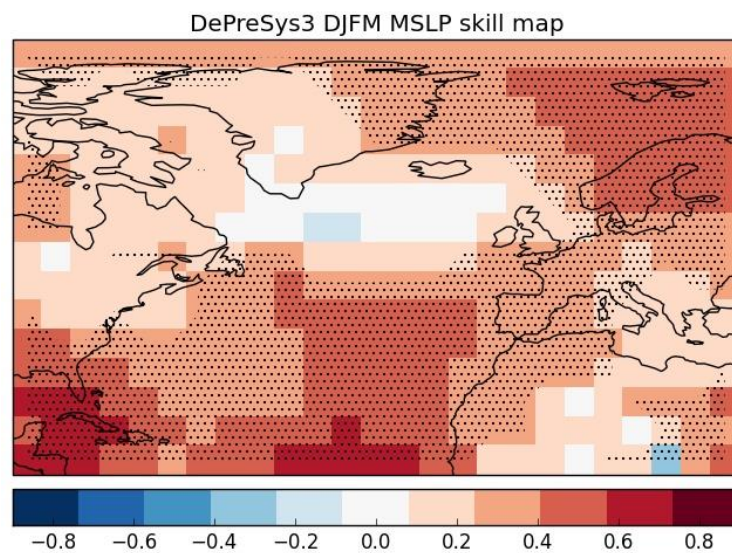


Figure 10. Spatial distribution of skill (correlation) for UK Met Office Decadal Climate Prediction System 3 (DePreSys3), predicting the season ahead winter (DJFM) mean sea level pressure. Stippled regions are significant at the 5% level according to a Student's t-test.

Acknowledgements

This research was funded by NERC through a Strategic Highlight Topics grant (Physical and biological dynamic coastal processes and their role in coastal recovery (BLUE-coast) NE/N015525/1). GD is supported by ESA under the Sea State CCI project, and by CNES under the CFOSAT-COAST project. BC funded by SONO (ANR-17-CE01-0014) through the Agence Nationale de la Recherche (ANR). The United Kingdom and Ireland directional wave climate data were from the UK Met Office 8-km WAVEWATCH III third-generation spectral wave model (version 3.14; Tolman, 2009). This dataset is not publicly available due to commercial restrictions, but can be sourced from the Met Office (enquiries@metoffice.gov.uk), co-author reference Dr Andrew Saulter) for specific research purposes. EOF-based climate indices used in

this study are publicly available for the period 1980–2017 (National Oceanic and Atmospheric Administration (NOAA) Climate Prediction Center; www.cpc.ncep.noaa.gov). The Western Europe Pressure Anomaly (WEPA) climate index (1943–2018) developed by Castelle et al. (2017) is publicly available online via the University of Plymouth PEARL open access research repository (<http://hdl.handle.net/10026.1/15509>). Season-ahead retrospective forecasts (hindcasts) of the winter-averaged December–March (DJFM) NAO and WEPA are not publicly available due to commercial restrictions, but can be sourced from the Met Office (enquiries@metoffice.gov.uk) for specific research purposes.

References

- Alpers, W.R., Ross, D.B., Rufenach, C.L., 1981. On the detectability of ocean surface waves by real and synthetic aperture radar. *Journal of Geophysical Research: Oceans* 86, 6481–6498. <https://doi.org/10.1029/JC086iC07p06481>
- Antolínez, J. A. A., Murray, A. B., Méndez, F. J., Moore, L. J., Farley, G., and Wood, J. (2018). Downscaling changing coastlines in a changing climate: The hybrid approach. *Journal of Geophysical Research: Earth Surface*, 123(2), 229–251
- Athanasiadis, P., Bellucci, A., Scaife, A. A., Hermanson, L., Materia, S., Sanna, A., Borrelli, A., MacLachlan, C. and Gualdi, S. (2016). A multi-system view of wintertime NAO seasonal predictions. *Journal of Climate*, 30, 1461–1475. doi:10.1175/JCLI-D-16-0153.1
- Baker, L. H., Shaffrey, L. C., Sutton, R. T., Weisheimer, A., & Scaife, A. A. (2018). An intercomparison of skill and overconfidence/underconfidence of the wintertime North Atlantic Oscillation in multimodel seasonal forecasts. *Geophysical Research Letters*, 45, 7808–7817. <https://doi.org/10.1029/2018GL078838>
- Barbosa, S., Silva, M. E., and Fernandes, M. J. (2006). Wavelet analysis of the Lisbon and Gibraltar North Atlantic Oscillation winter indices. *International Journal of Climatology*, 26(5), 581–593.
- Barnard, P. L., A. D. Short, M. D. Harley, K. D. Splinter, S. Vitousek, I. L. Turner, J. Allan, et al. (2015). Coastal Vulnerability across the Pacific Dominated by El Niño/Southern Oscillation, *Nature Geoscience* 8: 801–807.
- Barnston, A. G., Livezey, R. E., (1987) Classification, seasonality and persistence of low-frequency atmospheric circulation patterns. *Monthly Weather Review*, 115, 1083–1126.
- Bergillos, R.J., Ortega-Sánchez, M., Masselink, G., Losada, M.A. (2016). Morpho-sedimentary dynamics of a micro-tidal mixed sand and gravel beach, Playa Granada, southern Spain. *Marine Geology*. 379, 28–38.
- Burvingt, O., Masselink, G., Scott, T., Davidson, M., Russell, P. (2018). Climate forcing of regionally-coherent extreme storm impact and recovery on embayed beaches. *Marine Geology* 401, 112–128.
- Bromirski, P. D., Cayan, D. R., Helly, J., and Wittmann, P. (2013). Wave power variability

and trends across the North Pacific. *Journal of Geophysical Research: Oceans*, 118, 6329–6348.
<https://doi.org/10.1002/2013JC009189>

Buhler O. and T.E. Jacobson (2001). Wave-driven currents and vortex dynamics on barred beaches. *J. Fluid Mech.*, 449, 313–319.

Camus, P., Menéndez, M., Méndez, F. J., Izaguirre, C., Espejo, A., Cánovas, V., ... and Medina, R. (2014). A weather-type statistical downscaling framework for ocean wave climate. *Journal of Geophysical Research: Oceans*, 119(11), 7389–7405.

Castelle, B., Coco, G. (2012). The morphodynamics of rip channels on embayed beaches. *Continental Shelf Research*, 43, 10–23, doi: 10.1016/j.csr.2012.04.010.

Castelle, B., Marieu, V., Bujan, S., Ferreira, S., Parisot, J. P., Capo, S., et al. (2014). Equilibrium shoreline modelling of a high-energy meso-macrotidal multiple-barred beach. *Marine Geology*, 347, 85–94.

Castelle, B., Dodet, G., Dodet, G., Scott, T. (2017). A new climate index controlling winter wave activity along the Atlantic coast of Europe: the West Europe Pressure Anomaly. *Geophysical Research Letters*, 44, 1384–1392.

Castelle, B., Dodet, G., Masselink, G., and Scott, T. (2018). Increased winter-mean wave height, variability, and periodicity in the Northeast Atlantic over 1949–2017, *Geophysical Research Letters*, 45(8), 3586–3596.

Cazenave, A., Dieng, H.-B., Meyssignac, B., von Schuckmann, K., Decharme, B., Berthier, E. (2014). The rate of sea-level rise. *Nature Climate Change*, 4, 358–361, doi:10.1038/nclimate2159.

Colman, A. W., Palin, E. J., Sanderson, M. G., Harrison, R. T., & Leggett, I. M. (2011). The potential for seasonal forecasting of winter wave heights in the northern North Sea. *Weather and Forecasting*, 26(6), 1067– 1074.

Deser, C., Hurrell, J. W. and Phillips, A. S. (2017). The role of the North Atlantic Oscillation in European climate projections. *Climate Dynamics*, 49 (9), 3141—3157.

Dobrynin M, T. Kleine, A. Düsterhus and J. Baehr (2019). Skilful Seasonal Prediction of Ocean Surface Waves in the Atlantic Ocean. *Geophys. Res. Lett.*, 46, 1731– 1739.

Dodet, G., Bertin, X., Taborda, R. (2010). Wave climate variability in the North-East Atlantic Ocean over the last six decades. *Ocean Modelling* 31, 120–131.
<https://doi.org/10.1016/j.ocemod.2009.10.010>

Dodet, G., Castelle, B., Masselink, G., Scott, T., Davidson, M., Floe'h, F., Jackson, D., and Suanez, S. (2018). Beach recovery from extreme storm activity during the 2013/14 winter along the Atlantic coast of Europe. *Earth Surface Processes and Landforms*, 44 (1) 393–401.

Dunstone, N., Smith, D., Scaife, A. A., Hermanson, L., Eade, R., Robinson, N., et al.

(2016). Skilful predictions of the winter North Atlantic Oscillation one year ahead. *Nature Geoscience*, 9, 809–814.

Eade R., D. Smith, A.A. Scaife and E. Wallace, 2014. Do seasonal to decadal climate predictions underestimate the predictability of the real world? *Geophys. Res. Lett.*, 41, 5620–5628.

Harley, M.D., Turner, I.L., Short, A.D., Ranasinghe, R. (2011). A reevaluation of coastal embayment rotation: the dominance of cross-shore versus alongshore sediment transport processes, Collaroy-Narrabeen Beach, southeast Australia. *Journal of Geophysical Research: Earth Surface*, 116, 1–16.

Harley, M.D., I.L. Turner, M.A. Kinsela, J.H. Middleton, P.J. Mumford, K.D. Splinter, M.S. Phillips, J.A. Simmons, D.J. Hanslow, and A.D. Short. (2017). Extreme coastal erosion enhanced by anomalous extratropical storm wave direction. *Nature Scientific Reports* 7:6033.

CFOSAT: A New Mission in Orbit to Observe Simultaneously Wind and Waves at the Ocean Surface, 2019. . *Space Research Today* 206, 15–21.
<https://doi.org/10.1016/j.srt.2019.11.012>

Hurrell, J. W. (1995), Decadal Trends in the North Atlantic Oscillation: Regional Temperatures and Precipitation, *Science*, 269(5224), 676–679

Goodwin, I. D., Mortlock, T. R. and Browning, S. (2016). Tropical and extratropical-origin storm wave types and their influence on the East Australian longshore sand transport system under a changing climate. *Journal of Geophysical Research: Ocean*. 121, 4833–4853.

Grinsted, A., Moore, J. C., Jevrejeva, S. (2004). Application of the cross wavelet transform and wavelet coherence to geophysical time series. *Nonlinear Processes in Geophysics*, 11, 561566.

Itoh, H. (2008). Reconsideration of the true versus apparent Arctic Oscillation. *Journal of Climatology* 21(10): 2047–2062.

Kalnay, E., and Coauthors, (1996). The NCEP/NCAR 40-year Reanalysis Project. *Bulletin of the American Meteorological Society*, 77, 437-471.

Kim, H. M., Webster, P. and Curry, J. (2012). Seasonal prediction skill of ECMWF System 4 and NCEP CFSv2 retrospective forecast for the Northern Hemisphere winter. *Climate Dynamics* 23, 2957-2973.

Klein, A.H.D.F., Filho, L.B., Schumacher, D.H. (2002). Short-term beach rotation processes in distinct headland bay beach systems. *Journal of Coastal Research*, 18, 442–458.

Le Cozannet, G., Oliveros, C., Castelle, B., Garcin, M., Idier, D., Pedreros, R., Rohmer, J. (2016). Uncertainties in sandy shorelines evolution under the Bruun rule assumption. *Frontiers Marine Sciences*, 3, doi:0.3389/fmars.2016.00049.

- Ludka, B.C., Guza, R.T., O'Reilly, W.C. et al. (2019). Sixteen years of bathymetry and waves at San Diego beaches. *Scientific Data*, 6, 161, doi:10.1038/s41597-019-0167-6.
- Luterbacher, J., Schmutz, C., Gyalistras, D., Xoplaki, E., Wanner, H. (1999). Reconstruction of monthly NAO and EU indices back to AD 1675. *Geophysical Research Letters* 26, 2745–2748. <https://doi.org/10.1029/1999GL900576>.
- Luijendijk, A., Hagenaars, G., Ranasinghe, R., Baart, F., Donchyts, G., Aarninkhof, S. (2018). The State of the World's Beaches. *Scientific Reports*, 8(1), doi:10.1038/s41598-018-24630-6.
- Martinez-Asensio, A., Tsimplis, M. N., Marcos, M., Feng, X., Gomis, D., Jorda, G. and Josey, S. A. (2016). Response of the North Atlantic wave climate to atmospheric modes of variability *International Journal of Climatology*, 36 1210–25.
- Masselink, G., Castelle, B., Scott, T., Dodet, G., Suanez, S., Jackson, D., Floc'h, F. (2016). Extreme wave activity during 2013/2014 winter and morphological impacts along the Atlantic coast of Europe. *Geophysical Research Letters* 43: 2135–2143.
- McCarthy, G. D., Joyce, T. M. M., and Josey, S. A. (2018). Gulf Stream variability in the context of quasi-decadal and multidecadal Atlantic climate variability. *Geophysical Research Letters*, 45, 11,257–11,264. <https://doi.org/10.1029/2018GL079336>
- Mentaschi, L., Vousdoukas, M.I., Pekel, J.P., Voukouvalas, E., and Feyen, L. (2018). Global long-term observations of coastal erosion and accretion. *Scientific Report*, 8: 12876, doi:10.1038/s41598-018-30904-w.
- Mitchell, J. A., Bett, P. E., Hanlon, H. M., Saulter, A. (2017). Investigating the impact of climate change on the UK wave power climate. *Meteorologische Zeitschrift*.
- Montaño, J., Coco, G., Alvarez, J. A., Beuzen, T., Bryan, K., Cagigal, L., Castelle, B., Davidson, M., Goldstein, E., Ibaceta, R., Idier, D., Ludka, B., Masoud-Ansari, S., Méndez, F., Murray, A. B., Plant, N., Ratliff, K., Robinet, A., Rueda Z. A., and Vos, K. (2020). Blind testing of shoreline evolution models. *Scientific Reports*. 10. 10.1038/s41598-020-59018-y.
- Mortlock, T.R., Goodwin, I.D. (2016). Impacts of enhanced central pacific ENSO on wave climate and headland-bay beach morphology. *Continental Shelf Research*, 120, 14–25.
- Poli, P., Hersbach, H., Dee, D. P., Berrisford, P., Simmons, A. J., Vitart, F., et al. (2016). Era-20C: An atmospheric reanalysis of the twentieth century. *Journal of Climate*, 29(11), 4083–4097. <https://doi.org/10.1175/JCLI-D-15-0556.1>
- Ruiz de Alegria-Arzaburu, A., Masselink, G. (2010). Storm response and beach rotation on a gravel beach, Slapton Sands, U.K. *Marine Geology*. 278, 77–99.
- Santo, H., Taylor, P. H., Woollings, T., Poulson, S. (2015). Decadal wave power variability in the North-East Atlantic and North Sea. *Geophysical Research Letters* 42, 4956–4963. <https://doi.org/10.1002/2015GL064488>.

Saulter, A. (2015). Assessment of WAM Cycle-4 based source terms for the Met Office global-regional wave modelling system. Forecasting Research Technical Report 598, Met Office, Exeter, UK.

Scaife A.A., T. Spanghel, D. Fereday, U. Cubasch, U. Langematz, H. Akiyoshi, S. Bekki, P. Braesicke, N. Butchart, M. Chipperfield, A. Gettelman, S. Hardiman, M. Michou, E. Rozanov and T.G. Shepherd 2012. Climate Change and Stratosphere-Troposphere Interaction. *Clim. Dyn.*, 38, 2089-2097.

Scaife, A. A. et al. (2014). Skillful long-range prediction of European and North American winters. *Geophysical Research Letters*. 41, 2514–2519.

Scaife, A. A. and D. Smith, (2018). A signal-to-noise paradox in climate science. *NPJ: Climate and Atmospheric Science*, 1, <http://dx.doi.org/10.1038/s41612-018-0038-4>.

Scott, T., Masselink, G., Hare, T.O., Saulter, A., Poate, T., Russell, P., Davidson, M., Conley, D. (2016). The extreme 2013/2014 winter storms: beach recovery along the southwest coast of England. *Mar. Geol.* 382, 224–241.

Short, A.D., Masselink, G. (1999). Handbook of beach and shoreface morphodynamics. Embayed and Structurally Controlled Beaches. John Wiley.

Silva, A.N., Taborda, R., Bertin, X., Dodet, G. (2012). Seasonal to Decadal Variability of Longshore Sand Transport at the Northwest Coast of Portugal. *Journal of Waterway, Port, Coastal, and Ocean Engineering* 138, 464–472. [https://doi.org/10.1061/\(ASCE\)WW.1943-5460.0000152](https://doi.org/10.1061/(ASCE)WW.1943-5460.0000152)

Splinter, K. D., Davidson, M. A., Golshani, A., and Tomlinson, R. (2012). Climate Controls on Longshore Sediment Transport. *Continental Shelf Research* 48, 146–156.

Smith, D., Scaife, A. A., and Kirtman, B. (2012). What is the current state of scientific knowledge with regard to seasonal and decadal forecasting? *Environmental Research Letters*, 7, 015602.

Smith, D. M., Scaife, A. A., Eade, R. & Knight, J. R. (2016). Seasonal to decadal prediction of the winter North Atlantic Oscillation: emerging capability and future prospects. *Q. J. R. Meteorol. Soc.* 142, 611–617.

Smith, D. M., Eade, R., Scaife, A. A. et al. (2019). Robust skill of decadal climate predictions. *NPJ: Climate and Atmospheric Sciences*, 2 (13).

Tolman, H.L. (2009). User manual and system documentation of WAVEWATCH IIITM version 3.14. – NOAA/NWS/NCEP/ MMAB Technical Note 276, Environmental Modeling Center, Marine Modeling and Analysis Branch.

Turner, I. L., Harley, M. D., Short, A. D., Simmons, J. A., Bracs, M. A., Phillips, M. S., Splinter, K. D. (2016). A multi-decade dataset of monthly beach profile surveys and inshore wave forcing at Narrabeen, Australia, *Scientific Data*, vol. 3,

<http://dx.doi.org/10.1038/sdata.2016.24>

Vousdoukas, M.I., Mentaschi, L., Voukouvalas, E., Verlaan, M., Jevrejeva, S., Jackson, L.P., Feyen, L. (2018). Global probabilistic projections of extreme sea levels show intensification of coastal flood hazard. *Nature Communications*, 9: 2360, doi:10.1038/s41467-018-04692-w.

Wang, L., Ting, M., and Kushner, P. (2017). A robust empirical seasonal prediction of winter NAO and surface climate. *Scientific Reports*, 7(1), 279. <https://doi.org/10.1038/s41598-017-00353-y>

Ward, J. H. (1963). Hierarchical grouping to optimize an objective function, *Journal of the American Statistical Association*, 58, 236-244.

Wiggins, M. A., Scott, T., Masselink, G., Russell, P., and McCarroll, R. (2019a). Coastal embayment rotation: Response to extreme events and climate control, using full embayment surveys. *Geomorphology*, 327, 385-403.

Wiggins, M., Scott, T., Masselink, G., Russell, P., Valiente, N.G. (2019b). Regionally-Coherent Embayment Rotation: Behavioural Response to Bi-Directional Waves and Atmospheric Forcing. *Journal of Marine Science and Engineering*. 2019, 7, 116.

Woollings T, Hannachi A, Hoskins B. (2010). Variability of the North Atlantic eddy-driven jet stream. *Q. J. R. Meteorol. Soc.* 136(649): 856–868. <https://doi.org/10.1002/qj.625>.